Cadmium Stabilization Efficiency and Leachability by $CdAl_4O_7$ Monoclinic Structure

Minhua Su,[†] Changzhong Liao,[†] Kui-Hao Chuang,[‡] Ming-Yen Wey[§] and Kaimin Shih*[,†]

[†] Department of Civil Engineering, The University of Hong Kong, Pokfulam Road, Hong Kong

[‡] Department of Safety, Health, and Environmental Engineering, Central Taiwan University of Science and Technology, Taichung, Taiwan

[§] Department of Environmental Engineering, National Chung Hsing University, Taichung, Taiwan

Supporting Information

Including 2 tables and 8 figures over 10 pages

Table S1. Quantitative phase analysis results and the calculated transformation ratios (TR) of the authentic CdO : $CdAl_4O_7$: glass (amorphous) : CaF_2 determined via the Rietveld refinement method. The refinement was evaluated by the factors derived from the fitness criteria provided in Supporting Information Table S1.

Table S2. Weight variation of $CdAl_4O_7$ powder with or without calcination at 1025 ℃ for 3 h.

Figure S1. X-ray diffraction (XRD) patterns of the alumina powder (AlOOH, boemite; ICDD PDF no. 74-1895), γ-Al_2O_3 obtained by heating the alumina powder at 650°C for 3 h and the cadmium oxide powder (CdO, ICDD PDF no. 75-0594).

Figure S2. Schematic diagram of the cadmium stabilization reaction pathway with thermal treatment.

Figure S3. XRD patterns of the products obtained from the reaction of CdO + γ-Al_2O_3 with Cd/Al molar ratios of 2/1 and 3/4 heated at 1000 °C for 24 h. The standard patterns were derived from the International Centre for Diffraction Data (ICDD) database, including CdO (ICDD PDF no. 75-0594), $CdAl_4O_7$ (ICDD PDF no. 22-1061) and α-Al_2O_3 (ICDD PDF no. 74-1081).

Figure S4. A comparison of the observed (red cross symbol) and calculated XRD patterns (blue line) between 2θ = 28.75° and 30.00° in Figure 2 shows the unreported Bragg diffraction position (400) of the $CdAl_4O_7$ phase.

Figure S5. X-ray photoelectron spectroscopy (XPS) spectra for Cd 3d of (a) CdO and (b) $CdAl_4O_7$.

Figure S6. Particle size distributions of (a) CdO and (b) as-prepared $CdAl_4O_7$ powders for CPLT.

Figure S7. Decrease of the (a) Cd 3d signal and increase of the (b) Al 2p signal on the surface of the $CdAl_4O_7$ sample leached for 120 min and observed via X-ray photoelectron spectroscopy (XPS). The leaching process comprised the constant pH leaching test (CPLT) at pH 4.0 with nitric acid solution serving as the leaching fluid.

Figure S8. XRD patterns of the un-leached and leached (pH 4.0 for 120 min) $CdAl_4O_7$ samples. The comparison shows that both diffraction peaks were nearly identical and that no new crystalline phase was found after the CPLT process.

Table S1. Quantitative phase analysis results and the calculated transformation ratios (TR) of the authentic CdO : $CdAl_4O_7$: glass (amorphous) : CaF_2 determined via the Rietveld refinement method. The refinement was evaluated by the factors derived from the fitness criteria provided in Supporting Information Table S1.

Known		Refinement Results				
Composition (wt. %)	TR (%)	Composition (wt %)	TR (%)	GOF	R_p (%)	R_{wp} (%)
20.00 : 80.00 : 0.00 : 0.00	60.72	21.14 : 79.86 : -- : --	59.34	1.87	4.81	6.30
40.00 : 60.00 : 0.00 : 0.00	36.69	41.34 : 58.36 : -- : --	35.41	1.87	4.94	6.43
60.00 : 20.00 : 0.00 : 0.00	20.48	62.13 : 37.87 : -- : --	19.06	1.84	6.92	6.32
80.00 : 20.00 : 0.00 : 0.00	8.81	82.31 : 17.69 : -- : --	7.67	1.97	6.85	5.35
24.00 : 36.00 : 20.00 : 20.00	36.69	20.35 : 29.34 : 30.32 : 20.00	35.78	1.62	4.35	5.69
16.00 : 24.00 : 40.00 : 20.00	36.69	13.31 :19.56 : 47.13 : 20.00	36.22	1.65	4.54	5.96
36.00 : 24.00 : 20.00 : 20.00	20.48	31.75 : 19.38 : 28.87 : 20.00	19.08	1.75	4.76	6.25
24.00 : 16.00 : 40.00 : 20.00	20.48	20.41 : 12.93 : 46.66 : 20.00	19.67	1.71	4.71	6.14

"R-pattern", R_p, $R_p = \frac{\sum |Y_{o,m} - Y_{c,m}|}{\sum Y_{o,m}}$

"R-weight pattern", R_{wp}, $R_{wp} = \sqrt{\frac{\sum w_m (Y_{o,m} - Y_{c,m})^2}{w_m Y_{o,m}{}^2}}$

"R-expected", R_{exp}, $R_{exp} = \sqrt{\frac{\sum M - P}{\sum w_m Y_{o,m}{}^2}}$

"Goodness of fit", GOF, $GOF = \text{chi}^2 = \frac{R_{wp}}{R_{exp}} = \sqrt{\frac{\sum w_m (Y_{o,m} - Y_{c,m})^2}{M - P}}$

Table S2. Weight variation of $CdAl_4O_7$ powder with or without calcination at 1025 ℃ for 3 h.

Uncalcined $CdAl_4O_7$, g	Calcined $CdAl_4O_7$, g
1.0005	1.0003
1.0002	1.0001
1.0003	1.0004

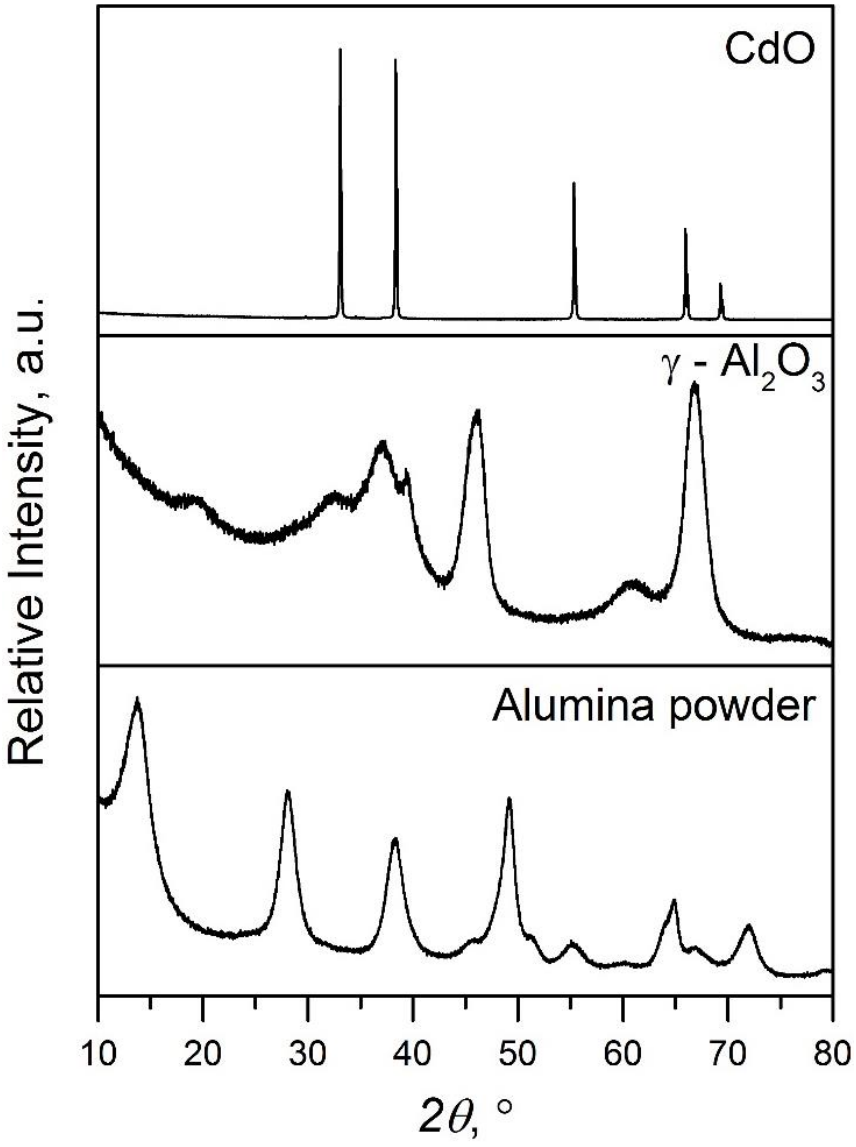

Figure S1. X-ray diffraction (XRD) patterns of the alumina powder (AlOOH, boemite; ICDD PDF no. 74-1895), γ-Al_2O_3 obtained by heating the alumina powder at 650°C for 3 h and the cadmium oxide powder (CdO, ICDD PDF no. 75-0594).

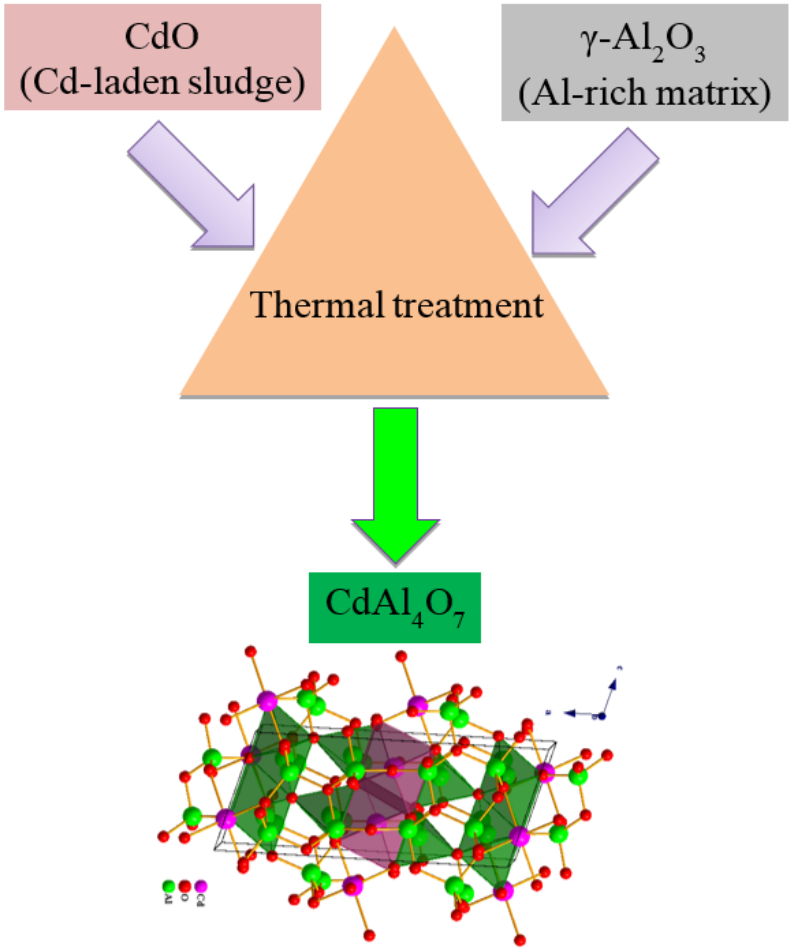

Figure S2. Schematic diagram of the cadmium stabilization reaction pathway with thermal treatment.

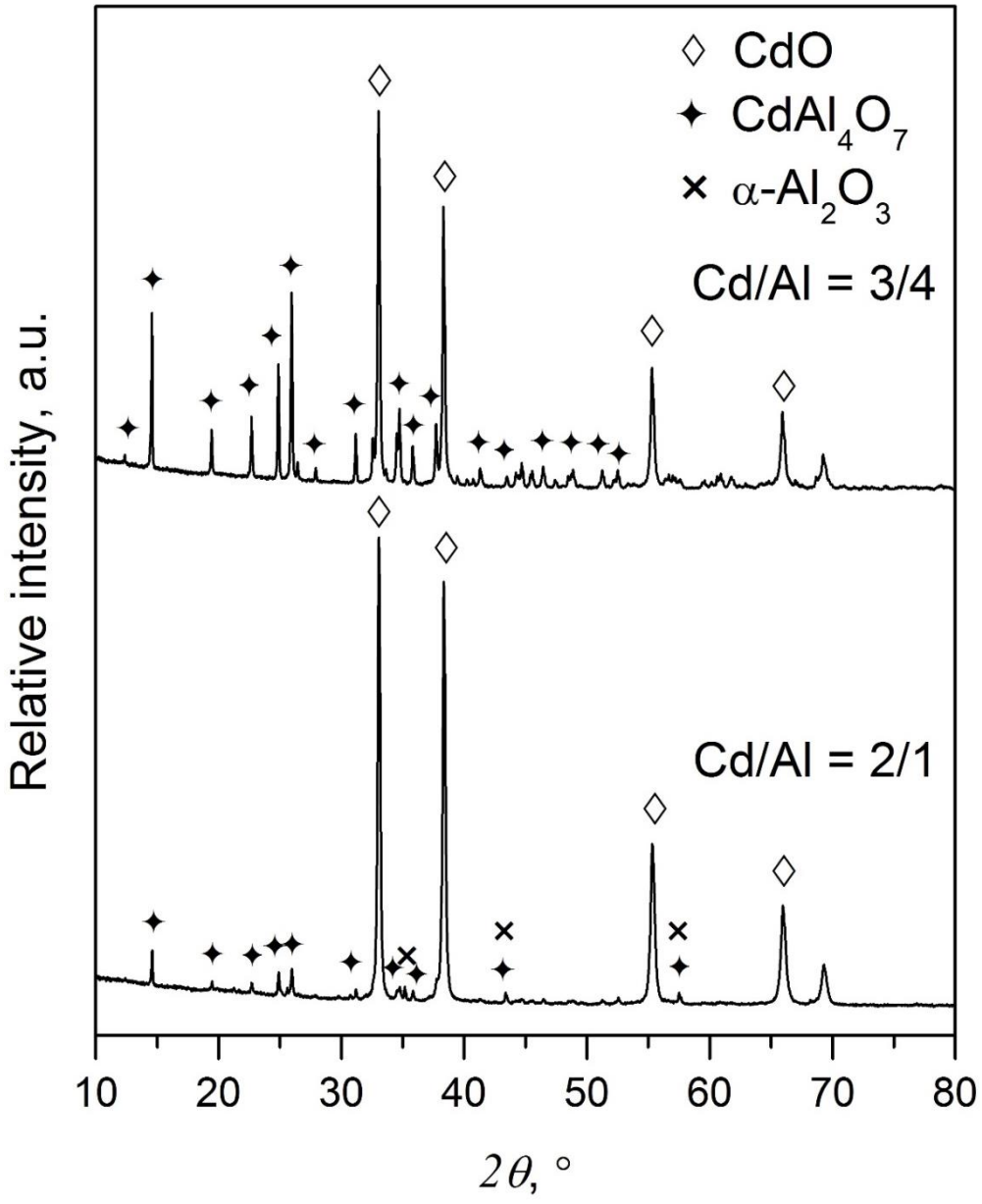

Figure S3. XRD patterns of the products obtained from the reaction of CdO + γ-Al_2O_3 with Cd/Al molar ratios of 2/1 and 3/4 heated at 1000 °C for 24 h. The standard patterns were derived from the International Centre for Diffraction Data (ICDD) database, including CdO (ICDD PDF no. 75-0594), $CdAl_4O_7$ (ICDD PDF no. 22-1061) and α-Al_2O_3 (ICDD PDF no. 74-1081).

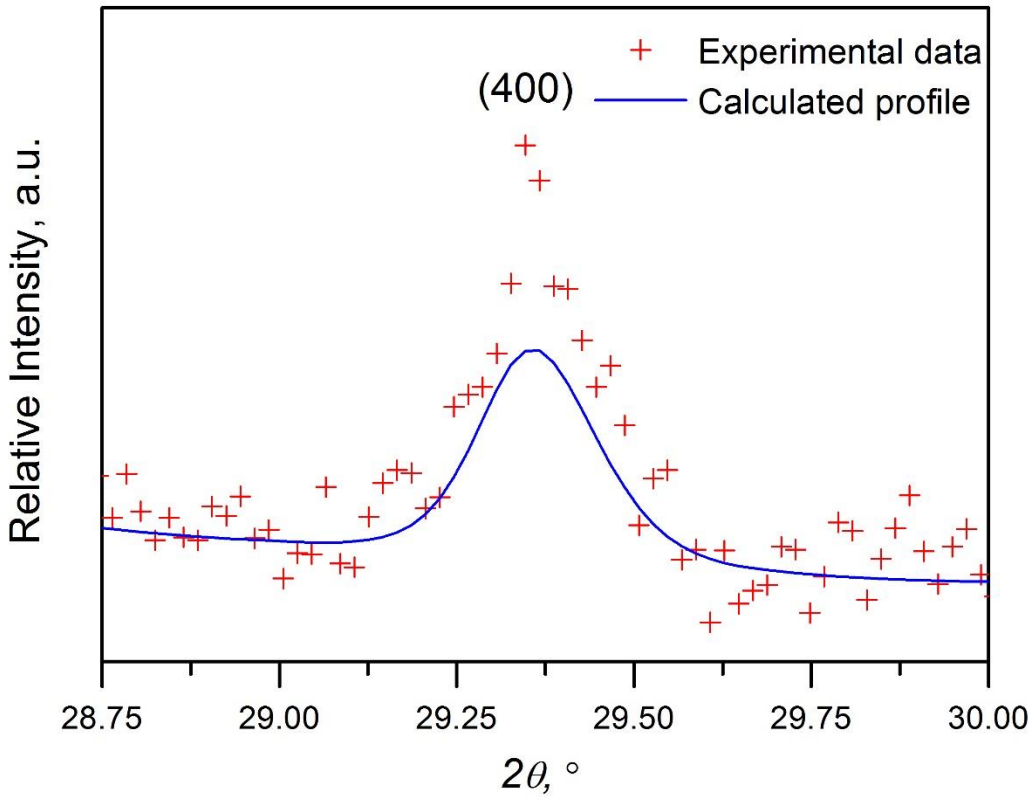

Figure S4. A comparison of the observed (red cross symbol) and calculated XRD patterns (blue line) between 2θ = 28.75° and 30.00° in Figure 2 shows the unreported Bragg diffraction position (400) of the $CdAl_4O_7$ phase.

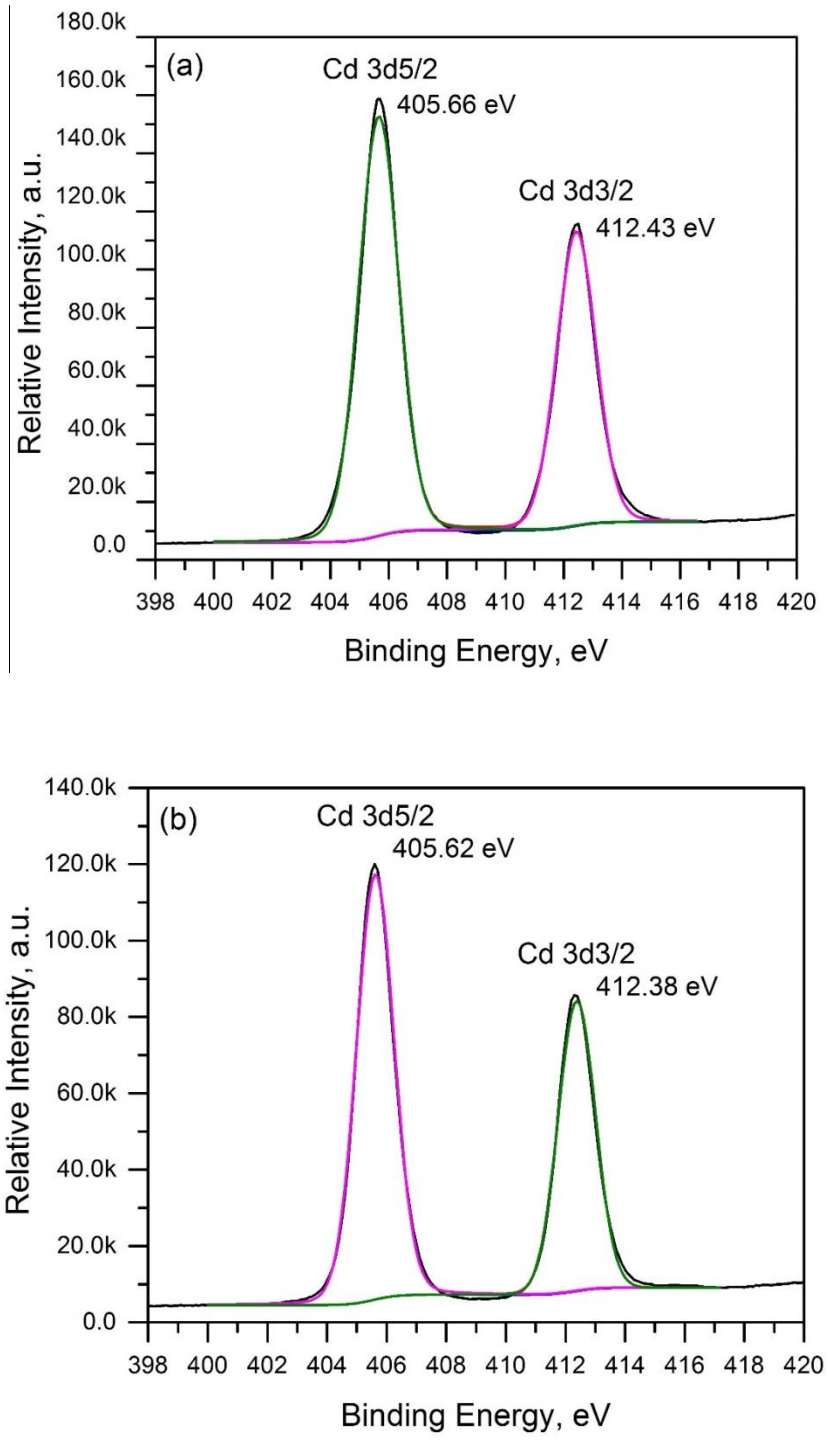

Figure S5. X-ray photoelectron spectroscopy (XPS) spectra for Cd 3d of (a) CdO and (b) $CdAl_4O_7$.

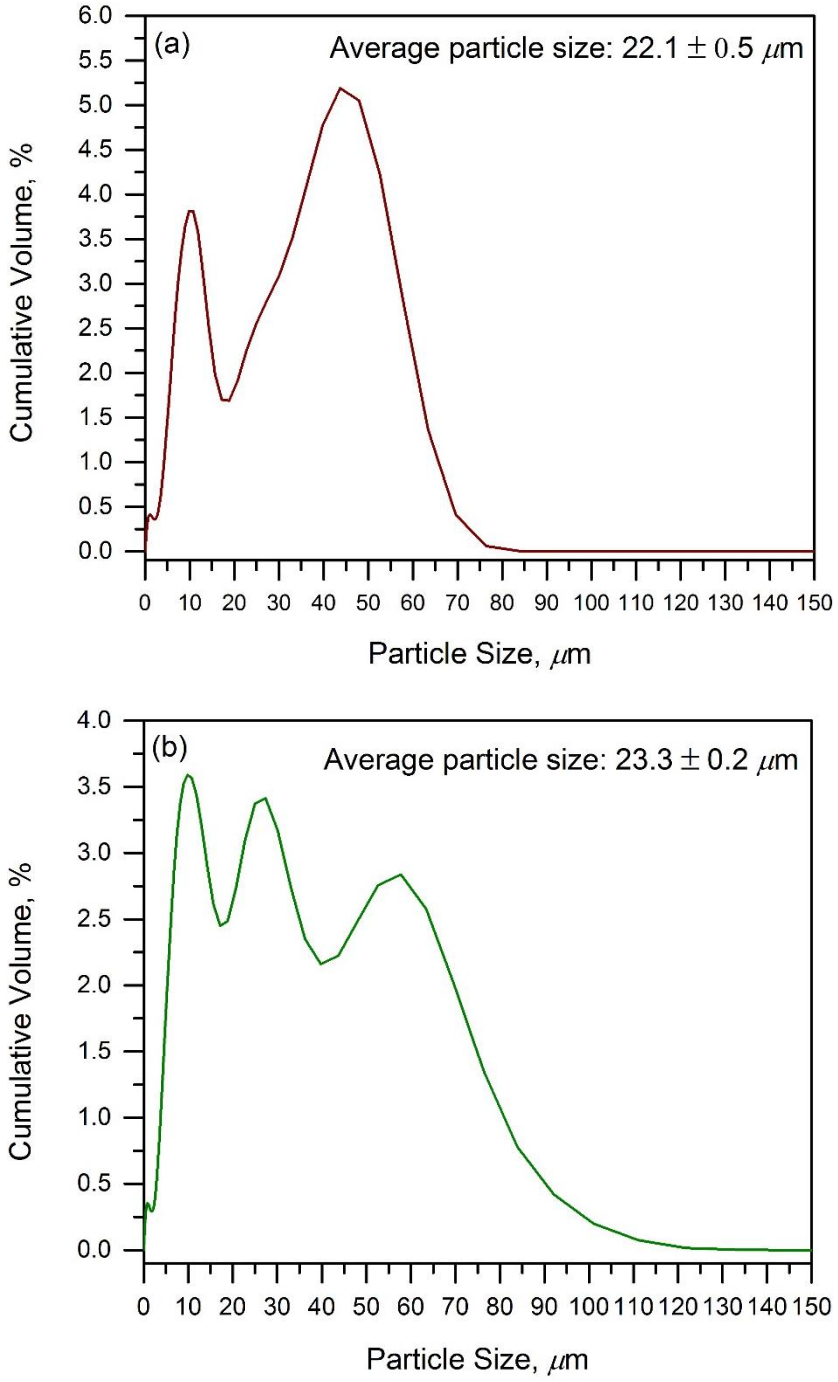

Figure S6. Particle size distributions of (a) CdO and (b) as-prepared $CdAl_4O_7$ powders for CPLT.

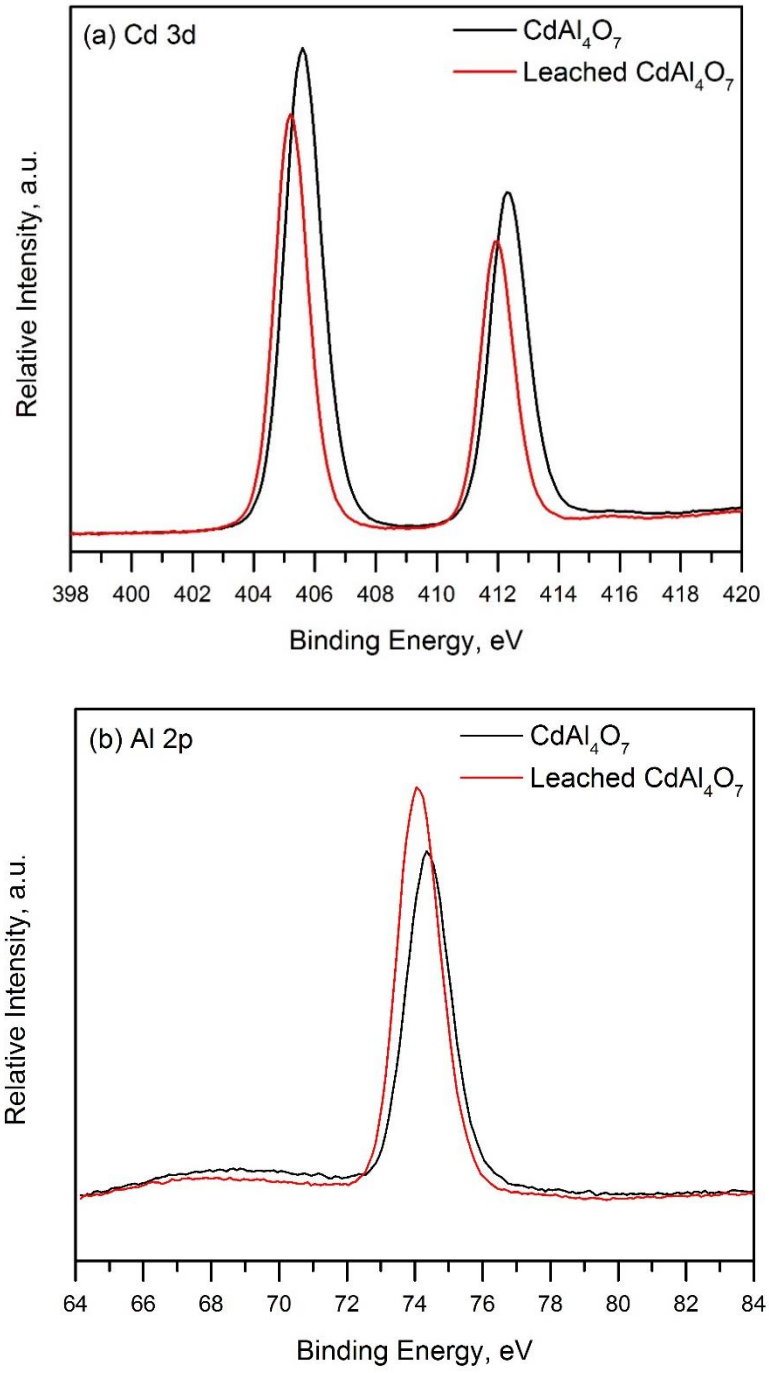

Figure S7. Decrease of the (a) Cd 3d signal and increase of the (b) Al 2p signal on the surface of the $CdAl_4O_7$ sample leached for 120 min and observed via X-ray photoelectron spectroscopy

(XPS). The leaching process comprised the constant pH leaching test (CPLT) at pH 4.0 with nitric acid solution serving as the leaching fluid.

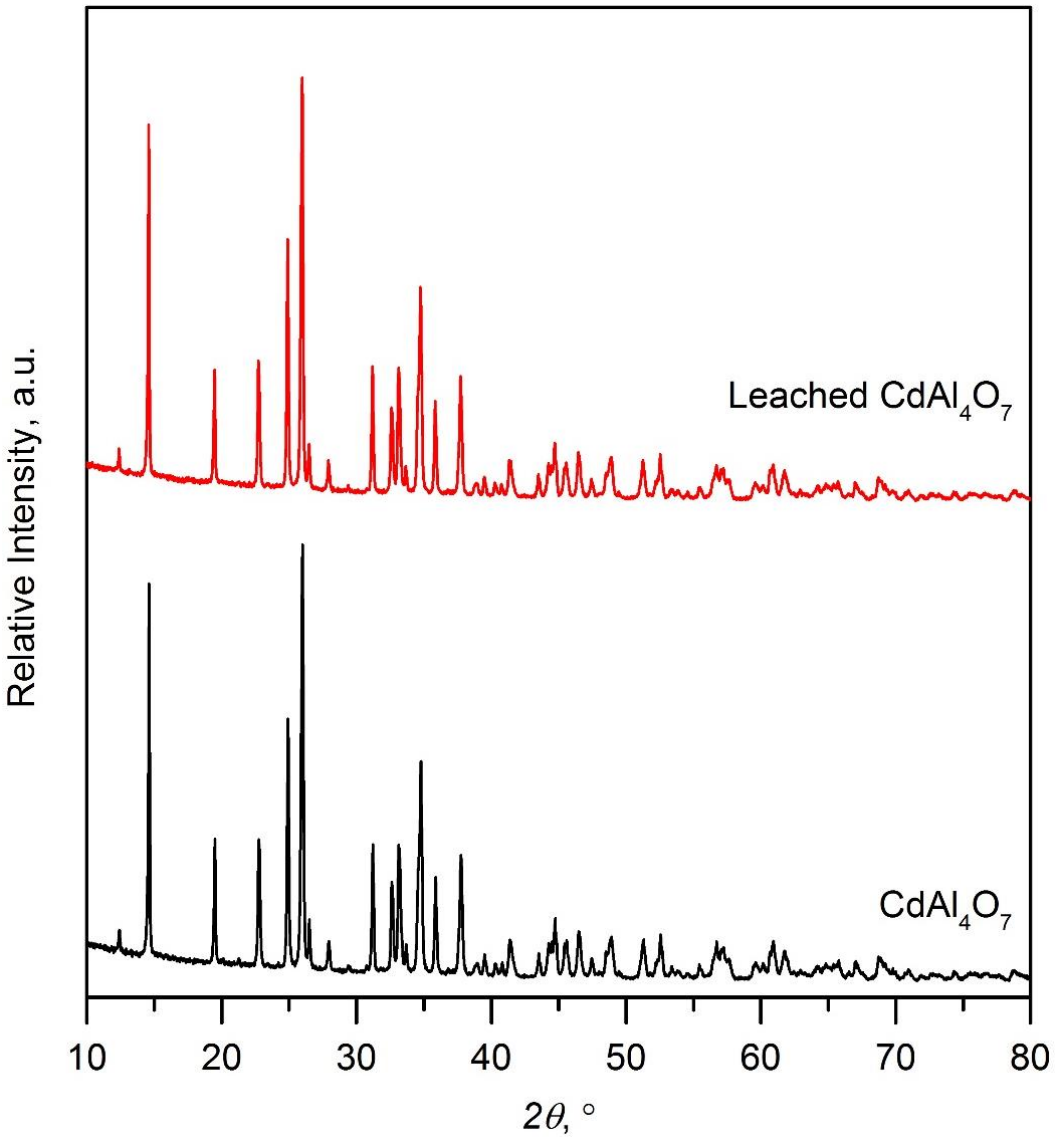

Figure S8. XRD patterns of the un-leached and leached (pH 4.0 for 120 min) $CdAl_4O_7$ samples. The comparison shows that both diffraction peaks were nearly identical and that no new crystalline phase was found after the CPLT process.